



Study of field-induced phase transitions in 0.68PbMg₁/3Nb₂/3O₃–0.32PbTiO₃ relaxor single crystal by polarized micro-Raman spectroscopy

Chao Chen, Hao Deng, Xiaobing Li, Haiwu Zhang, Ting Huang, Di Lin, Sheng Wang, Xiangyong Zhao, Zhigao Hu, and Haosu Luo

Citation: *Applied Physics Letters* **105**, 102909 (2014); doi: 10.1063/1.4894418

View online: <http://dx.doi.org/10.1063/1.4894418>

View Table of Contents: <http://scitation.aip.org/content/aip/journal/apl/105/10?ver=pdfcov>

Published by the [AIP Publishing](#)

Articles you may be interested in

[Determination of full set material constants of \[011\]c poled 0.72Pb\(Mg₁/3Nb₂/3\)O₃-0.28PbTiO₃ single crystal from one sample](#)

Appl. Phys. Lett. **105**, 012901 (2014); 10.1063/1.4886765

[Kinetics and thermodynamics of the ferroelectric transitions in PbMg₁/3Nb₂/3O₃ and PbMg₁/3Nb₂/3O₃-12% PbTiO₃ crystals](#)

J. Appl. Phys. **113**, 184104 (2013); 10.1063/1.4804069

[Structural transitions in \[001\]/\[111\]-oriented 0.26Pb\(In₁/2Nb₁/2\)O₃-0.46Pb\(Mg₁/3Nb₂/3\)O₃-0.28PbTiO₃ single crystals probed via neutron diffraction and electrical characterization](#)

J. Appl. Phys. **113**, 154104 (2013); 10.1063/1.4802669

[Domain engineered switchable strain states in ferroelectric \(011\) \[Pb\(Mg₁/3Nb₂/3\)O₃\]_{\(1-x\)}-\[PbTiO₃\]_x \(PMN-PT, x0.32\) single crystals](#)

J. Appl. Phys. **109**, 124101 (2011); 10.1063/1.3595670

[Micro-Raman study of the microheterogeneity in the M A-M C phase transition in 0.67PbMg₁/3Nb₂/3O₃-0.33PbTiO₃ single crystal](#)

J. Appl. Phys. **109**, 083517 (2011); 10.1063/1.3574666

The logo for AIP Chaos is displayed on a red background with a geometric, low-poly pattern. The letters 'AIP' are in a large, white, sans-serif font, followed by a vertical bar and the word 'Chaos' in a smaller, white, sans-serif font.

CALL FOR APPLICANTS
Seeking new Editor-in-Chief

Study of field-induced phase transitions in 0.68PbMg_{1/3}Nb_{2/3}O₃–0.32PbTiO₃ relaxor single crystal by polarized micro-Raman spectroscopy

Chao Chen,^{1,2,3,a)} Hao Deng,^{1,3} Xiaobing Li,¹ Haiwu Zhang,^{1,3} Ting Huang,⁴ Di Lin,¹ Sheng Wang,¹ Xiangyong Zhao,¹ Zhigao Hu,⁴ and Haosu Luo^{1,a)}

¹Key Laboratory of Inorganic Functional Materials and Devices, Shanghai Institute of Ceramics, University of Chinese Academy of Sciences, 215 Chengbei Road, Jiading, Shanghai 201800, China

²Department of Materials Science and Engineering, Jiangxi Key Laboratory of Advanced Ceramic Materials, Jingdezhen Ceramic Institute, Jingdezhen 333001, China

³University of Chinese Academy of Sciences, Beijing 100049, China

⁴Department of Electronic Engineering, East China Normal University, Shanghai 200241, People's Republic of China

(Received 15 July 2014; accepted 20 August 2014; published online 12 September 2014)

Polarized Raman spectroscopy has been performed to investigate the effects of the electric field on 0.68PbMg_{1/3}Nb_{2/3}O₃–0.32PbTiO₃ (PMN–32PT) relaxor single crystal. Based on the group theory analysis, the Raman modes of PMN–32PT single crystal at zero-field are assigned to the monoclinic structure. The electric-field-evolution of Raman spectra reveal that a structural transition to tetragonal phase is initiated at a threshold electric field E_1 and completed at higher field E_2 . In the intermediate field range from E_1 to E_2 , the structure of the crystal is determined to be a coexistence of monoclinic and tetragonal phases. These results of the Raman spectra allow us to better understand the field-induced ultrahigh macroscopic strain in the relaxor ferroelectrics. © 2014 AIP Publishing LLC.

[<http://dx.doi.org/10.1063/1.4894418>]

Relaxor-based ferroelectric single crystals such as $(1-x)\text{Pb}(\text{Zn}_{1/3}\text{Nb}_{2/3})\text{O}_3-x\text{PbTiO}_3$ (PZN– x PT) and $(1-x)\text{Pb}(\text{Mg}_{1/3}\text{Nb}_{2/3})\text{O}_3-x\text{PbTiO}_3$ (PMN– x PT) have attracted much attention due to their superior piezoelectric properties compared to commercial piezoelectric ceramics (PZT). For example, the PMN–PT single crystals with composition near the morphotropic phase boundary (MPB) exhibit the ultrahigh piezoelectric response ($d_{33} = 2500$ pC/N) along the [001]-direction.^{1,2} Extensive studies on these materials have demonstrated a monoclinic phase in the MPB region is response for their excellent piezoelectric properties.^{3–5} In fact, an electric(E)-field induced intermediate monoclinic phase between the rhombohedral(R)–tetragonal(T) phase transition was observed by Noheda *et al.*^{5,6} in PZN-PT single crystal. However, Zhang *et al.*⁷ have proposed that the monoclinic phase does not directly contribute to the ultrahigh piezoelectric activity in PMN–PT crystal. The role of monoclinic phase (M) is thought to form R – M or M – T phase boundaries, corresponding to an ease in polarization rotation under external E -field. Therefore, it is crucial to investigate the effects of E -field on the monoclinic structure of PMN–PT single crystals to further understand the outstanding electromechanical properties in these materials.

Raman spectroscopy is considered to be a sensitive technique for studying local lattice dynamics and phase transitions in relaxor ferroelectric crystals.^{8–16} The anomalies of Raman active-mode are strongly associated with phase transitions. Moreover, the light couples directly with the ferroelectric polarization make it useful in study of lattice dynamics. Polarized Raman spectroscopy has been done

for monoclinic PMN–PT single crystal. The field-induced M_C -type to the M_A -type monoclinic phase transition was identified at low E -field ($E = 5.8$ kV/cm).¹⁶ However, the E -field dependent Raman measurement on PMN–PT has not yet been presented across M – T phase transition. It is of interest to examine the differences in the phonon behaviors near and during this M – T transition. In this letter, polarized Raman scattering is performed on the PMN–32PT single crystal under a broad fields range from 0 to 22.3 kV/cm. The results clearly show that the E -field applied in the [001]-direction induces a phase transition from the M phase at low fields ($E < 10.0$ kV/cm) to the T phase at high fields ($E > 16.3$ kV/cm) through a phase coexistence region in the intermediate fields.

The PMN–32PT single crystal was grown by a modified Bridgman technique.¹⁷ Pseudocubic crystal orientation was determined using x -ray diffraction. The dimensions of the samples are $4 \times 4 \times 0.4$ mm³ with two main faces perpendicular to [001]-direction. The two (100) faces of samples were optically polished and coated with semitransparent gold electrodes for E -field application. Raman spectra were recorded in backscattering configuration using a Jobin-Yvon LabRAM HR 800 UV spectrometer with a 488 nm line of an Ar⁺ laser as the exciting source. The spectra were recorded in parallel (VV) $z(xx)\bar{z}$ and cross (VH) $z(xy)\bar{z}$ polarization geometries, where x , y , and z are the cubic axes. The laser beam was focused through a $50\times$ microscope with a working distance of 18 mm. An air-cooled charge coupled device (CCD) with a 1024×256 pixels front illuminated chip was used to collect the scattered signal dispersed on 1800 grooves/mm grating.

Figure 1 shows the polarized Raman spectra for [001]-oriented PMN–32PT single crystal at zero field. It can be

^{a)}Author to whom correspondence should be addressed. Electronic mail: cc2762@163.com and hsluo@mail.sic.ac.cn

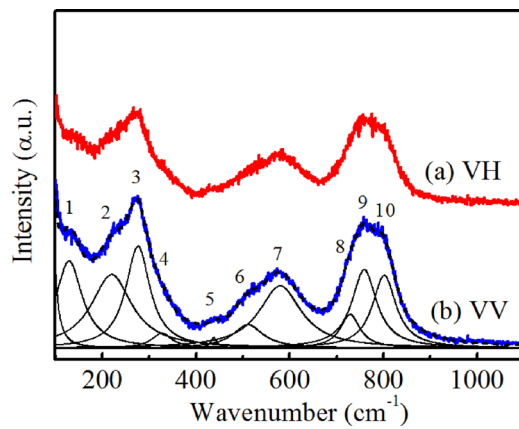


FIG. 1. Polarized Raman spectra of PMN-32PT single crystal at zero-field, and the deconvolution of multiple Lorentzian peaks are shown for the VV scattering geometry.

seen that the cross (VH) and parallel (VV) Raman spectra do not differ qualitatively except for the intensity variations. This effect is probably ascribed to the existence of micropolar domains, which partly influences the vibrational properties, as well as the Raman selection rules.^{8,18} To better ascertain the locations and the number of Raman modes, the Raman spectra are decomposed into Lorentzian-shaped peaks. The deconvoluted spectrum is displayed in the VV geometry and ten modes are discernible in the frequency range of 100–1000 cm^{-1} . We noted that, in Ref. 12, four additional modes in the range of 0–100 cm^{-1} were detected for PMN-32PT crystal. However, the edge filters used in present experiment do not allow us to observe these low-frequency modes (e.g., <100 cm^{-1}). This indicates that the number of the modes in sample should be more than ten. Based on the group theory analysis, there are twelve Raman active modes classified as $8A'$ and $4A''$ in the monoclinic (Pm) symmetry, while only seven Raman modes are predicted in the rhombohedral ($R3m$) structure and eight modes in tetragonal structure ($P4mm$).^{11,12} Thereby, it is suggested that the room temperature structure of unpoled PMN-32PT single crystal belongs to monoclinic. The discrepancy of mode numbers between the experiment and theory analysis in PMN-PT compound can be explained by the existence of the polar nanoregions in relaxor ferroelectrics.¹³

Although the zero-field Raman spectra in the VV geometry are similar to those in the VH geometry, they are distinguished from each other as the E -field is increased. One dominant feature is the changing of the intensities of modes at 146, 580, and 760 cm^{-1} . From the spectra in the VH geometry (Fig. 2(a)), these modes decrease in their intensity upon increasing E -field. Nevertheless, the opposite trend is observed in the VV geometry (Fig. 2(b)). These changes are clearly exhibited in Fig. 3(a), where the intensities ratio ($I_{\text{VH}}/I_{\text{VV}}$) of 146, 580, and 760 cm^{-1} mode are plotted against applied E -field. The ratio of the modes makes an abrupt change as field reaches 10.0 kV/cm, and further increasing of the field brings about another notable change. It is worthy that these changes in intensity ratio are consistent with the E -field versus strain curve (Fig. 3(b)). A rapid increase of strain appears at a threshold field strength E_1 of about 10.0 kV/cm, and a slope change is observed

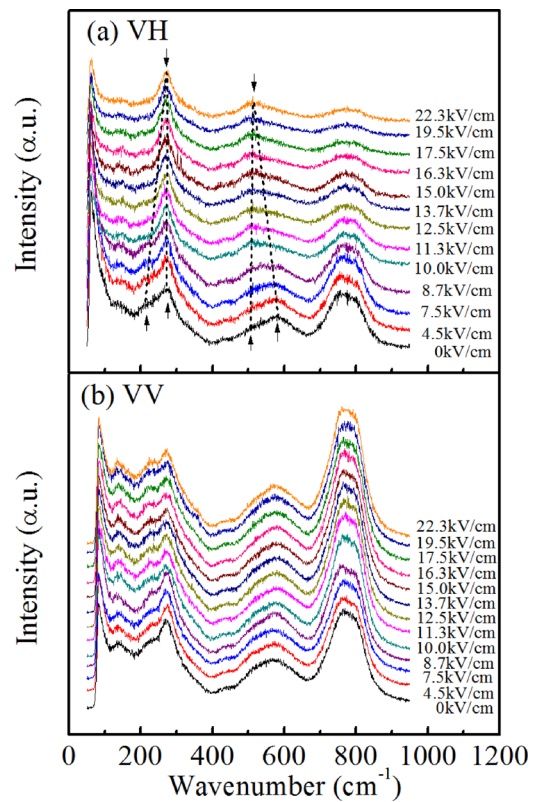


FIG. 2. Room temperature Raman spectra in the VH scattering geometry (a) and VV scattering geometry (b) under various electric fields.

with increasing field to E_2 (about 16.3 kV/cm). Thus, the coincidence of our Raman data and macroscopic strain measurements indicates that the structural phase transitions actually occur across two critical fields E_1 and E_2 .

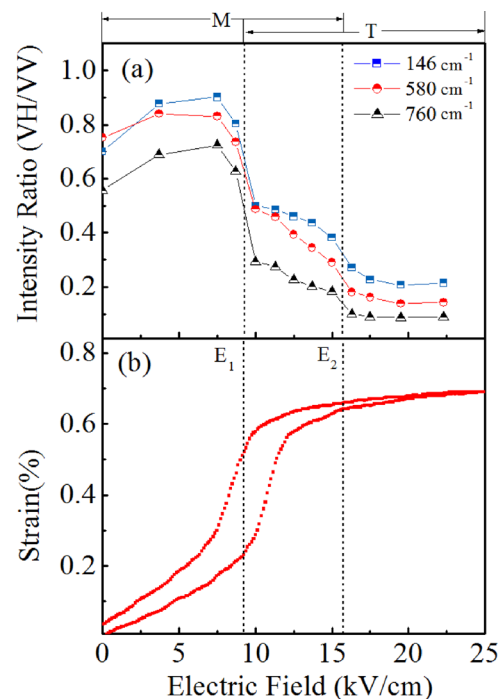


FIG. 3. The field evolution of the intensity ratio of the VH to VV component of the 146, 580, and 760- cm^{-1} modes (a); and the longitudinal strain (b) for [001]-oriented PMN-32PT crystal as functions of the applied electric fields.

Except for the variation of the mode intensity, some features such as frequency shift and mode merging are observed in the E -field induced Raman spectra (Fig. 2(a)). These features are typical for perovskite relaxor ferroelectrics. As presented in Fig. 2(a), the mode at 210 cm^{-1} exhibits a clear blueshift and has a tendency to merge into the mode at 274 cm^{-1} , leading to the reduction in the number of Raman modes. From the viewpoint of group theory analysis, the point group C_s of the monoclinic phase is a subgroup of C_{4v} of the tetragonal phase. When the monoclinic-tetragonal (M - T) phase transition takes place, the $A' \oplus A''$ modes in the monoclinic phase will transform into E mode of the tetragonal structure.^{11,14,15} Thus, the decline of Raman modes may reveal a change in symmetry to tetragonal phase with a lower number of Raman active modes. The similar phenomenon has also been found in the M - T transition of PZT materials.¹⁴ On the other hand, we observe an apparent frequency shift in the modes around 580 cm^{-1} . Upon increasing the E -field, the mode at 580 cm^{-1} gradually merges into the mode at 504 cm^{-1} , making its frequency shift become 525 cm^{-1} . According to the mode assignment in previous studies,^{14,19,20} the mode at about 525 cm^{-1} in the VH geometry is assigned to the E (3TO) phonon mode in the tetragonal symmetry. This fact gives additional support to the transition from the monoclinic to the tetragonal phase, though the mode vibrational mechanism is thought to be more complicated at a lower symmetry structure.²¹ It should be noted that these E -field dependent spectra are quite similar to the PZN-8PT Raman spectra observed during the M - T phase transition induced by temperature.¹⁸

Previous Raman studies on Pb-based relaxors have showed that the M - T phase transition occurred at a temperature point in the temperature-dependent Raman spectra.^{12,18} It is noteworthy that these changes across the critical temperature are comparable to the changes across the lower transition field (E_1) in the E -field dependence Raman spectra (Fig. 2). On the other hand, the upper transition field (E_2) is identified in the E -field induced intensity ratio behavior (Fig. 3(a)). Additionally, the changes across E_2 are not as obvious as those across E_1 . This suggests that the field-induced phase transition from M to T phase is initiated at E_1 and completed above E_2 , corresponding to a rapid increase and a saturation of the strain (Fig. 3(b)), respectively. In other words, the phase structure of the sample is actually a mixture of the M and T phases between E_1 and E_2 . This is consistent with the earlier interpretation reported by Noheda *et al.*, who suggested that monoclinic and tetragonal phases coexist in an intermediate field region from their x -ray-diffraction measurements.⁶

In order to verify this fact, we assume that the mixing ratio of one phase at an intermediate E -field (E_m) is proportional to the difference from the E_1 with respect to the difference of $E_2 - E_1$. Then the Raman spectra at E_m could be represented by a linear superposition of the spectra below E_1 and above E_2 . As presented in Fig. 4, the fitted Raman spectra in the VV and VH geometries, respectively, at E_m of 12.5 kV/cm are displayed in comparison with the observed spectra at the same field. The fitted spectra are obtained from the linear superposition of the Raman spectra at E_1 and E_2 followed by

$$\{\text{FIT}\} = (1 - r) \times \{\text{MCS}\} + r \times \{\text{TGS}\}, \quad (1)$$

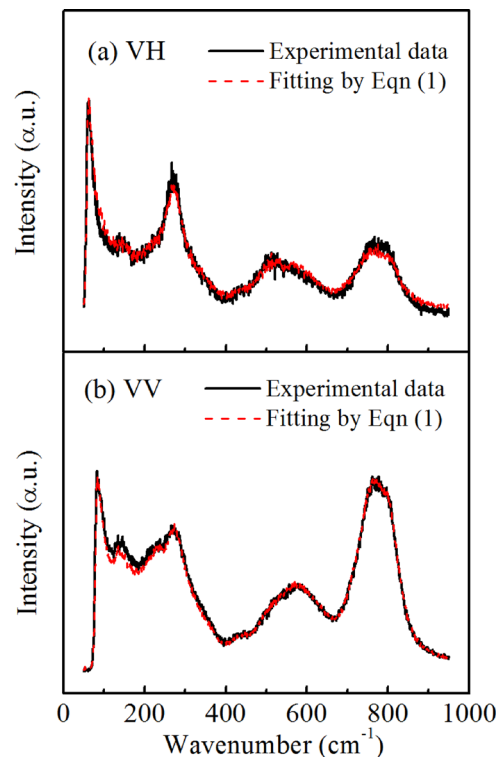


FIG. 4. Fitted Raman spectra of (a) VH and (b) VV scattering geometry, in comparison with the observed Raman spectra of the PMN-32PT crystal at one arbitrary intermediate electric field of 12.5 kV/cm .

where $\{\text{FIT}\}$ represents the fitted Raman spectra, $r = (E_m - E_1)/(E_2 - E_1)$, $\{\text{MCS}\}$ Raman spectrum of the monoclinic phase, and $\{\text{TGS}\}$ Raman spectrum of the tetragonal phase. The coincidence of the experimental and the fitted Raman spectra is excellent for both VV and VH geometries, which strongly confirmed the coexistence of the monoclinic and tetragonal phases in the intermediate field range from E_1 to E_2 .

In summary, polarized Raman spectroscopy performed on monoclinic PMN-32PT crystals show that an electric field applied along $[001]$ -direction induces the tetragonal phase. Our experiments reveal that such a phase transition is initiated at E_1 (about 10.0 kV/cm), and completed at about E_2 (about 16.3 kV/cm). Between E_1 and E_2 , both monoclinic and tetragonal phase coexist in PMN-32PT crystal. These results are in good agreement with the E -field strain curves, which strongly support for this sequence of the phase transitions.

This work was financially supported by the Ministry of Science and Technology of China through 973 Program (No. 2013CB632900), the Natural Science Foundation of China (Nos. 61001041, 11090332, and 51272268), Science and Technology Commission of Shanghai Municipality (No. 12DZ0501000), Shanghai Rising-Star Program (No. 11QA1407500).

¹S.-E. Park and T. R. Shrout, *J. Appl. Phys.* **82**, 1804 (1997).

²S. E. Park and T. R. Shrout, *Mater. Res. Innovations* **1**, 20 (1997).

³R. R. Chien, V. H. Schmidt, C. S. Tu, and F. T. Wang, *J. Cryst. Growth* **292**, 395 (2006).

⁴C. S. Tu, C. M. Hsieh, V. H. Schmidt, R. R. Chien, and H. Luo, *Appl. Phys. Lett.* **93**, 172905 (2008).

- ⁵B. Noheda, D. E. Cox, G. Shirane, S.-E. Park, L. E. Cross, and Z. Zhong, *Phys. Rev. Lett.* **86**, 3891 (2001).
- ⁶B. Noheda, Z. Zhong, D. E. Cox, and G. Shirane, *Phys. Rev. B* **65**, 224101 (2002).
- ⁷F. Li, S. J. Zhang, Z. Xu, X. Y. Wei, J. Luo, and T. R. Shrout, *J. Appl. Phys.* **108**, 034106 (2010).
- ⁸S. Kim, I. S. Yang, J. K. Lee, and K. S. Hong, *Phys. Rev. B* **64**, 094105 (2000).
- ⁹J. Toulouse, F. Jiang, O. Svitelskiy, W. Chen, and Z.-G. Ye, *Phys. Rev. B* **72**, 184106 (2005).
- ¹⁰S. Kamba, E. Buixaderas, J. Petzelt, J. Fousek, J. Nosek, and P. Bridenbaugh, *J. Appl. Phys.* **93**, 933 (2003).
- ¹¹A. Slodczyk, A. Kania, and P. Daniel, *Phase Transitions* **79**, 399 (2006).
- ¹²A. Slodczyk, P. Daniel, and A. Kania, *Phys. Rev. B* **77**, 184114 (2008).
- ¹³M. El Marssi and H. Dammak, *Solid State Commun.* **142**, 487 (2007).
- ¹⁴J. Frantti, V. Lanto, S. Nishio, and M. Kakihama, *Jpn. J. Appl. Phys., Part 1* **38**, 5679(1999).
- ¹⁵K. C. V. Lima, A. G. S. Filho, A. P. Ayala, J. M. Filho, P. T. C. Freire, F. E. A. Melo, E. B. Araujo, and J. A. Eiras, *Phys. Rev. B* **63**, 184105 (2001).
- ¹⁶Y. Yang, Y. L. Liu, S. Y. Ma, K. Zhu, L. Y. Zhang, J. Cheng, G. G. Siu, Z. K. Xu, and H. S. Luo, *Appl. Phys. Lett.* **95**, 051911 (2009).
- ¹⁷H. S. Luo, G. S. Xu, H. Xu, P. Wang, and Z. Yin, *Jpn. J. Appl. Phys., Part 1* **39**, 5581 (2000).
- ¹⁸J. Cheng, Y. Yang, Y. H. Tong, S. B. Lu, J. Y. Sun, K. Zhu, Y. L. Liu, G. G. Siu, and Z. K. Xu, *J. Appl. Phys.* **105**, 053519 (2009).
- ¹⁹G. Burns and B. A. Scott, *Phys. Rev. B* **7**, 3088 (1973).
- ²⁰K. K. Mishra, A. K. Arora, S. N. Tripathy, and D. Pradhan, *J. Appl. Phys.* **112**, 073521 (2012).
- ²¹M. Iwata, H. Hoshino, H. Orihara, H. Ohwa, N. Yasuda, and Y. Ishibashi, *Jpn. J. Appl. Phys., Part 1* **39**, 5691 (2000).